JCTC Journal of Chemical Theory and Computation

PERSPECTIVE

pubs.acs.org/JCTC

Finding Reaction Pathways of Type A + B → X: Toward Systematic Prediction of Reaction Mechanisms

Satoshi Maeda*,†,‡ and Keiji Morokuma*,‡,§

†The Hakubi Center, Kyoto University, Kyoto 606-8302, Japan

‡Fukui Institute for Fundamental Chemistry, Kyoto University, Kyoto 606-8103, Japan

§Department of Chemistry and Cherry L. Emerson Center for Scientific Computation, Emory University, Atlanta, Georgia 30322, United States

Supporting Information

ABSTRACT: In these five decades, many useful tools have been developed for exploring quantum chemical potential energy surfaces. The success in theoretical studies of chemical reaction mechanisms has been greatly supported by these tools. However, systematic prediction of reaction mechanisms starting only from given reactants and catalysts is still very difficult. Toward this goal, we describe the artificial force induced reaction (AFIR) method for automatically finding reaction paths of type A + B → X (+ Y). By imposing an artificial force to given reactants and catalysts, the method can find the reactive sites very efficiently. Further pressing by the artificial force provides approximate transition states and product structures, which can be easily reoptimized to the corresponding true ones. This procedure can be executed very efficiently just by minimizing a single function called the AFIR function. All important reaction paths can be found by repeating this cycle starting from many initial orientations. We also discuss perspectives of automated reaction path search methods toward the above goal.

I. INTRODUCTION

Finding reaction paths as well as underlying transition states (TSs) has been one of the primary tasks in theoretical studies of the chemical reaction mechanism. Transition state is a key concept in the transition-state theory (TST),[1] in which the reaction path is introduced rather abstractly as paths connecting a reactant and a product through a TS. By early development of semiempirical and ab initio theories, TS structures began to be located explicitly as first-order saddle points on potential energy surfaces (PESs).[2−6] The intrinsic reaction coordinate (IRC) was introduced in 1970 as the center line of idealized reaction paths, defined as a mass-weighted steepest descent path starting from a first-order saddle point.[7] Calculation of IRC on the basis of an ab initio theory was accomplished in 1977,[8] by the development of the analytical gradient method,[9,10] and paths for the HNC → HCN and H^- + CH_4 → CH_4 + H^- reactions were the first examples of ab initio IRCs. Many useful tools have since been developed for finding TSs and IRCs,[11,12] and by using such tools, numerous reaction mechanisms have been elucidated.[13−16]

It should be noted that our focus in this paper is on local chemical bond rearrangements involving a few to several tens of atoms. Global optimization, conformation sampling, crystal structure sampling, etc.,[17−23] are outside the scope of this paper.

Once a TS is obtained, the associated IRC can nowadays be computed automatically by using one of the advanced steepest descent path integration methods.[8,24−27] The most complicated step is locating the TS. A variety of geometry optimization techniques, such as the gradient minimization,[4] the Berny optimization,[28,29] the eigenvector following (EF),[30] the geometry direct inversion in the iterative subspace,[31] and the rational function optimization[32] (RFO), have been a great help to locate the exact saddle point starting from a guessed TS structure. When estimating a TS geometry and/or a reaction mechanism, qualitative chemical theories, such as the frontier molecular orbital (FMO) theory[33,34] and the Woodward−Hoffmann rules,[35,36] are very helpful and have been frequently considered. TS optimization often requires a very good initial guess. Hence, results may depend on the provided guess. It may happen that important paths are missed in the search, if one fails to provide a proper guess of the corresponding TS geometry. An absence of an important path may cause serious disagreement between a theoretical conclusion and experimental data. Moreover, a theoretical prediction may be meaningless by the lack of a single important path. Therefore, an automated search that does not rely on any initial guess is desired for reliable determination as well as prediction of the reaction mechanism.

In many cases, one knows both a reactant and a product. Thus, double-end approaches are very useful to look for the TS(s) and a minimum energy path connecting the known end points. There have been considerable efforts for developing such approaches, e.g., the synchronous transit method,[37] the saddle optimization method,[38] the self-penalty walk method,[39] the nudged elastic band (NEB) method,[40] the string method,[41] the growing string method,[42] and others.[11,12] These double-ended methods considerably reduced the difficulty concerned with the initial guess of TS. However, these methods usually assume at first that the reaction path connects these two points along the straight line and tend to provide to a path closest to this straight line. Hence, it is not guaranteed that the most important (in general the lowest)

Received: April 27, 2011
Published: June 24, 2011

ACS Publications © 2011 American Chemical Society

path is obtained when there is more than one path. This problem can be avoided by providing appropriate intermediate geometries if available. In other words, double-end methods usually require a guess of reaction mechanism, that is, a series of important geometries, including a reactant, a product, and some key intermediates as well.

There are some methods which can find a reaction path automatically starting with only the reactant if reaction variables are given. The single coordinate driving (SCD), which has frequently been employed since very early studies of reaction paths,[5,6] was employed also in automated path sampling.[43] The metadynamics[44] method is very powerful in calculations of free energy barriers for given reaction variables and has been successfully applied to many problems, including chemical reactions.[45] The fast marching method can very quickly give a minimum energy path for a given set of reaction variables.[46] Although no input of product or TS is necessary in these methods, one has to select a small number of well-chosen, chemically relevant collective variables. In this sense, these methods also require a guess of reaction mechanism.

There are several approaches completely free from the issue of initial guess. Three such methods, the gradient extremal following (GEF) method,[47−56] the reduced gradient following (RGF, also called Newton trajectory) method,[57−63] and the anharmonic downward distortion following (ADDF) method,[64−66] were applied to global mapping of the whole topography of the PES of H_2CO on the basis of quantum mechanical calculations. These methods automatically located all local minima and TSs relevant to all chemical bond rearranging reactions, i.e., $H_2CO \leftrightarrow H_2 + CO$, $H_2CO \leftrightarrow HCOH$, $HCOH \leftrightarrow H_2 + CO$, $HCOH \leftrightarrow COH_2$, and $COH_2 \leftrightarrow H_2 + CO$, starting from the local minimum of H_2CO.[56,57,65] Thus, these methods have the ability to find all paths for unimolecular reactions automatically. However, the former two are computationally too expensive to be applied to systems larger than H_2CO. Only the ADDF method has been practically used successfully in global reaction route mapping for systems consisting of ∼10 atoms.[67] Several options are available in the ADDF method regarding applications to larger systems and nonadiabatic reactions.[68−70] There are some valley filling type approaches, such as the isopotential contour following[71] method and the chemical flooding[72] method. These can find only a single reaction path starting from a valley of a given reactant molecule, although this single path often corresponds to the lowest barrier path.

The goal of this study is development of a tool by which all important reaction paths can be obtained automatically just by providing multiple reactant species. Reactions among them, denoted A + B → X (+ Y) type in this paper, are of essential importance in organic chemistry, where B can be a catalyst. Nevertheless, among the above fully automated search methods without any initial guess, the only practical ones, the ADDF method as well as the valley filling methods are designed to find paths of type A → X (+ Y) starting from local minima. Global optimization, conformation sampling, cluster structure sampling, etc. usually treat paths of type A → X, e.g., protein folding occurring between two conformers of a peptide. Hence, methods successfully applied to such a problem are not readily applicable to paths of type A + B → X. Although there are shallow potential minima of weak complexes between A and B, such potential wells are often located in very floppy regions of PES, far away from TSs for bond reorganization. Since topology of PES involved in initial association states between A and B is very different from that in the product minimum of X, a method specially suited for such systems needs to be developed.

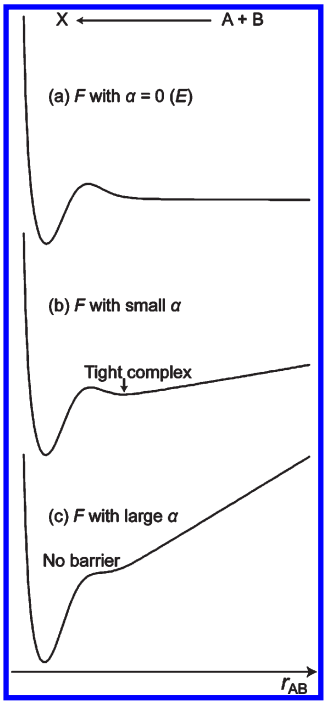

Figure 1. $F(\mathbf{Q})$ in eq 1: (a) with α = 0, (b) with small α, and (c) with large α.

Recently, we have developed a method capable of solving the present problem.[73] The idea is pretty simple; just pressing given reactant molecules to each other by a constant force. Hence, we call the method the artificial force induced reaction (AFIR) method. We have applied this method to an organic multicomponent reaction and to nonadiabatic spin flipping reactions[74,75] and have demonstrated that the method has the ability to discover unexpected reaction paths automatically and systematically. In this paper, the AFIR method is described in detail. The reason why the method works very well in the automated reaction path search is illustrated with a very simple application to the reaction $CO_2 + H \rightarrow HCO_2/HOCO$. An application to the reaction between vinyl alcohol (H_2C = CH−OH) and formaldehyde (H_2CO), which has an implication to the aldol reaction, provided automatically many reaction pathways including the aldol reaction among others. As case studies of three and four component reactions, one or two water molecules were added to these reactants as potential molecular catalysts, and many paths involving the water molecule(s) as aproton-transfer agent were located. Finally, perspectives of automated reaction path search methods are discussed.

II. THEORY

AFIR Method. In the AFIR method,[73] two or more reactants are pressed to each other by a constant force. At first, it is illustrated for the simplest case in which both A and B are single atoms. A constant force can be applied between A and B just by adding a linear function of distance r_{AB} to the potential energy function $E(r_{AB})$:

$$F(r_{AB}) = E(r_{AB}) + \alpha r_{AB} \quad (1)$$

where α is a parameter of the strength of the force. Figure 1a−c shows the function of eq 1 with α = 0 and with small and large α, respectively, for a typical diatomic potential energy curve $E(r_{AB})$. Along the curve in Figure 1a, there is a reaction barrier separating the reactant region A + B and the well of the product X. By imposing a weak force in Figure 1b, a local minimum for a tight complex is generated before the barrier. With a strong force, the barrier disappears, and the curve in Figure 1c is fully attractive. On $F(r_{AB})$ in Figure 1c, one can find the product X just by minimizing the function starting from A + B.

In designing a general representation of the force term for a system with multiple degrees of freedom, one should take into account some requirements: the function should be uniquely defined (automatically determined) at all geometries, the function should be differentiable up to the second order, and the function should not change anisotropies of each reactant as much as possible. The third requirement suggests that a best function would be as a sum of isotropic functions centered at each atom. Hence, we proposed the following AFIR function:

$$F(\mathbf{Q}) = E(\mathbf{Q}) + \alpha \frac{\sum_{i \in A} \sum_{j \in B} [(R_i + R_j)/r_{ij}]^p r_{ij}}{\sum_{i \in A} \sum_{j \in B} [(R_i + R_j)/r_{ij}]^p} \quad (2)$$

where $E(\mathbf{Q})$ is the PES that depends on the atomic coordinates $\mathbf{Q} = \{Q_k\}$, r_{ij} is a distance between the ith and jth atoms, and summations are taken over all pairs of atoms in the reactants A and B. Chemical bond reorganization usually occurs in a local reaction center. Thus, the inverse distance weighting[76] is employed so that the force is imposed only to closely interacting pairs, where p is a parameter (set to the standard value: $p = 6$) of the weight. In this weight, each inverse distance is scaled by the sum of covalent radii $(R_i + R_j)$ of the ith and jth atoms, respectively, to take the difference in atomic size into account.

The parameter α for the strength of force can be rewritten as

$$\alpha = \frac{\gamma}{\left[2^{-1/6} - \left(1 + \sqrt{1 + \frac{\gamma}{\varepsilon}}\right)^{-1/6}\right] R_0} \quad (3)$$

This equation represents an average force acting on two atoms in the energy range $0 < E < \gamma$,when E is formally represented by the Lennard-Jones potential (although the method is insensitive to what form of potential is used). The parameter γ is a model collision energy between two reactant particles; in the following and also in previous studies, γ is used instead of α for convenience. In practice we adopted R_0 and ε to be the values for argon clusters (R_0 = 3.8164 Å and ε = 1.0061 kJ/mol).

A minimization of $F(\mathbf{Q})$ gives an approximate structure for a product X starting from a reactant pair A + B. The minimization path of $F(\mathbf{Q})$ is called the AFIR path, along which an approximate TS geometry can be obtained as a highest point of $E(\mathbf{Q})$. Such an approximate TS geometry is then used as an initial guess for full optimization of the true TS geometry without the artificial force. Although eq 2 is the functional form we presently adopt, further improvements of the functional form might increase the efficiency and the accuracy in the future.

Algorithm. A flowchart of the automated search is shown in Figure 2. Four kinds of information are required in the input: a set of (separately optimized) reactant structures, a set of quantum chemical parameters (computation level, total charge, spin multiplicity, etc.), a maximum model collision energy γ_{MAX} value (see below), and a stopping criterion N_{MAX} (also see below). γ_{MAX} essentially controls the highest energy that is searched in the present method. A choice of small value of γ_{MAX} restricts the search to the low-energy region that can be reached with the model collision energy γ_{MAX}, and the search is less expensive. On the other hand, a large value of γ_{MAX} forces the search to high-energy regions, and the search is more exhaustive but is more expensive. In the present study, the AFIR minimization is performed starting from many random orientations, although more systematic ways or use of an intuitive orientation for a known mechanism can also be considered.

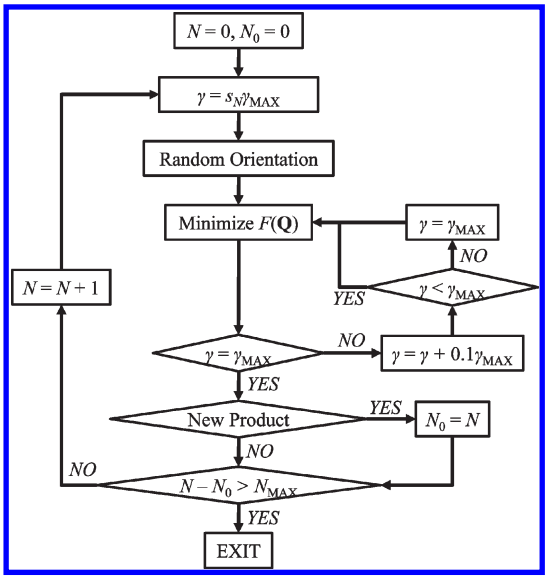

Figure 2. A flowchart of the automated reaction path search by the AFIR method.

At the first step of the Nth cycle, the model collision energy γ (see eq 3) is set to $s_N\gamma_{MAX}$, where s_N is a random number in the range: {0,1}. Then, a random orientation of the reactant species is generated. $F(\mathbf{Q})$ is minimized starting from the selected random orientation. Once all convergence criteria (maximum absolute gradient g_{MAX}, root-mean-square gradient g_{rms}, maximum absolute displacement d_{MAX}, root-mean-square displacement d_{rms}) are met, γ is compared to γ_{MAX}. If $\gamma < \gamma_{MAX}$, then γ is increased by $0.1\gamma_{MAX}$, and minimization of $F(\mathbf{Q})$ is repeated with the updated γ starting from the latest geometry. Once a local minimum with $\gamma = \gamma_{MAX}$ is obtained, the structure is examined: (1) If no new chemical bond is seen between the reactant species, then the structure is discarded, (2) if the structure is already found in a previous cycle, then the structure is discarded, or (3) the structure is registered to a list of products, and N_0 is updated to N. This cycle is repeated while $N - N_0 \leq N_{MAX}$.

A parallel implementation of this algorithm is very easy; just distributing each minimization task (from the $\gamma = s_N\gamma_{MAX}$ step to the $N = N + 1$ step in Figure 2) to each CPU core. In this study, we actually implemented this procedure in parallel.

The AFIR method is implemented in a local developmental version of the GRRM program.[64−66] The minimum search was performed by using the RFO method.[32] When a step size of the RFO method exceeded a given trust radius d_{TR} (about the control of d_{TR} is discussed below), the minimization step was replaced by a step of the trust radius method,[77] which gives a

quasi-Newton step of the size d_{TR}. In this study, the exact Hessian matrix was computed in every 50 minimization steps and was updated by the BFGS[78−81] method, which is the default setting of the GRRM program and can be changed by users. The convergence criteria, i.e., g_{MAX}, g_{rms}, d_{MAX}, and d_{rms}, were set to 6.0×10^{-5} hartree Å^{-1}, 4.0×10^{-5} hartree Å^{-1}, 3.0×10^{-4} Å, and 2.0×10^{-4} Å, respectively, in the final optimization with $\gamma = \gamma_{MAX}$. Looser criteria with 10 times these values were used when $\gamma < \gamma_{MAX}$. All optimized structures without the artificial force, i.e., true TSs and true products, also met the tighter optimization criteria, where the RFO optimizer implemented in the GRRM program was employed in the TS optimization as well as in the product geometry optimization.

The initial random geometries were generated as follows:

(A) Determine the random orientation of all the fragments:
  (1) Make three random vectors with their origins at the center-of-mass of one fragment.
  (2) These vectors are orthonormalized.
  (3) The three vectors are considered as new *xyz* axes and the original geometry is represented by the new axes.
  (4) perform steps 1 to 3 for all the fragments.

(B) Now determine the random positions of the centers-of-mass of all the fragments:
  (1) Among M fragments, one fragment is selected randomly and its center-of-mass position is placed at the origin.
  (2) Then, another fragment is chosen randomly from the remaining $M - 1$ fragments; this second fragment is placed at a random position around the first fragment. Since this procedure may put two fragments too close to each other, the center-of-mass position of the second fragment is moved randomly (with a step size of 0.05 Å) until the minimum distance from the first fragment exceeds a threshold (the sum of the covalent radii plus 0.8 Å).
  (3) Repeat this procedure for the third, fourth, .. and the last fragments.

There are some technical subtleties for a better implementation of this algorithm. The treatment starting with small γ and gradually increasing it by $0.1\gamma_{MAX}$ is one of these. With this trick, one can set the γ_{MAX} parameter to a relatively large value so that many reaction paths with a variety of barrier heights can be obtained in one search. For low-barrier paths, a very large γ allows the AFIR minimization to pass through a high-energy region far from the corresponding true TS. Hence, the smaller γ tends to give a better approximate TS. When the same product is reached, the maximum energy point along the previous path is compared with the one along the present path, and then, the path with a lower barrier is retained and the other is discarded. With this trick, a good approximate TS is obtained along low-barrier AFIR paths even if γ_{MAX} is very large.

Another point to consider in order to obtain a good approximate TS is a proper control of the trust radius d_{TR} around the TS region. In optimization of an energy minimum, the maximum and minimum values of d_{TR} are set to 0.5 and 0.001 Å, respectively. Between these values, d_{TR} is controlled as follows: When an optimization step increased the function value, d_{TR} is scaled by 0.1, and when the function value is decreased, d_{TR} is scaled by 3.0. Although this step control works well for usual energy minimization, there have been some troubles in the AFIR minimization. Before a barrier, direction of the artificial force and that of the true potential force are opposite, giving a normal norm of the total force. After passing through the barrier, these two vectors suddenly direct to the same direction, and the norm of the total force becomes too large. This sometimes causes an abnormal jump of atoms involved in the bond rearrangement, making a bump on the potential energy profile along the AFIR path. Hence, when an optimization step gave a structure containing new chemical bonds and when the step changed lengths of the new bonds more than 5%, d_{TR} is reduced to 0.05 Å, and the optimization step is recalculated, where atoms i and j with a distance shorter than $1.2(R_i + R_j)$ were considered to be bonded in this study. With this trick, AFIR paths can be calculated very efficiently by the energy minimization method with a relatively large step size used in usual geometry optimization in other regions.

The final point is a special treatment of hydrogen (H) atoms in eq 2. As discussed in Section III, the artificial force accentuates the short-range orbital interactions so that sites with maximal orbital interactions appear as local minima on the AFIR function. Existence of long-range interactions, such as H-bonds, is explicitly seen as local minima even on bare $E(\mathbf{Q})$. In other words, reactive sites for hydrogen-/proton-transfer reactions can be found by energy minimization without the artificial force. Hence, we set the covalent radius parameter R in the weight function for H atoms to zero. It should be emphasized that this does not mean that hydrogen-/proton-transfer paths are omitted. Entrances of hydrogen-/proton-transfer paths can be found as local minima even if the weight is small. Once such a H-bond site is located, the artificial force is imposed to H atoms even if $R = 0$, and a hydrogen-/proton-transfer reaction occurs. Without this treatment, AFIR minimization with small γ frequently falls into H-bond sites because of the long-range H-bond interaction. In order to efficiently find reactive sites for bond formations between heavy atoms with small γ, this treatment is recommended.

General Remarks. The present method may be categorized into the bias potential approaches.[82−85,44] Such methods have been used for accelerating molecular dynamics as well as global optimization. The common idea is to eliminate unwanted local minima using bias potentials constructed by unique mathematical procedures and data collected by extensive PES sampling. However, these methods may not be very effective in the present purpose. Strategies for eliminating flat regions of PESs for weakly interacting reactants should be very different from those for eliminating closed valleys. Hence, the bias employed in the present study is not similar to those for the previous approaches.

What is the best bias potential to eliminate the flat regions of PESs? A variety of functions, such as the harmonic, the Morse, and the Gaussian functions, may be possible candidates. The use of the linear function αr_{AB} in eq 1 was considered by assuming collisions among reactant molecules. In collisions, the driving force to overcome a reaction barrier is the inertia force to keep the translation of reactant molecules toward the TS. Hence, we chose to impose the (model inertia) force using the linear function. The force completely changes the landscape of the PES; the flat asymptote is completely eliminated by the linear function bias, as seen in Figure 1c.

One significant advantage of the present method is that the bias potential is defined uniquely at any given geometry without prior sampling of PES. This advantage arises from a single assumption in the AFIR method that a part of reactant species is connected with chemical bonds in the product. In this sense,

the present method is in part related to previous methods that assume a product structure or a small set of reaction variables.[37−46] However, the assumption in the AFIR method is much more flexible than those. Consequently, many reaction paths giving unexpected products through unexpected reaction variables are discovered in the AFIR method. In other words, AFIR is essentially a single-end method starting from given reactants as this single assumption does not specify which product will be found. More importantly, no empirical guess of the mechanism is required in the AFIR method.

We acknowledge two methods are especially related to AFIR. One is SCD[5,6,43] (and its modern form of RGF).[57−63] If the force is applied between a pair of atoms k and l (when $F(r_{kl}) = E(r_{kl}) + \alpha r_{kl}$ is minimized), then the minimization path should be very similar to the path followed by SCD for r_{kl}. Another is the steered molecular dynamics,[86] which applies a force to specified atoms to accelerate a particular event in molecular dynamics or to simulate single-molecule experimental techniques, such as atomic force microscopy and optical tweezers. The uniqueness of AFIR is that the direction of the force or the driving coordinate(s) is automatically given by eq 2. Among the numerous possible directions of the force or the huge combinations of the coordinates, eq 2 can choose suitable ones automatically, which enables an automated search. Despite the automatic selection of the driving coordinates, there are few AFIR paths wandering into dead end valleys without any reaction, which is demonstrated in Section IV.

Although we discussed only technical aspects of the AFIR method above, there is another important effect of the artificial force, that is, accentuate the local quantum chemical (frontier orbital) interactions leading to a TS. This helps finding an entrance of reaction paths in the automated search. In other words, the use of an artificial force to push the reactants together is no more than a starting point. After many trails and errors in adjusting the form of the force term, we discovered a special function (AFIR function) on which all reactive sites among multiple reactants can be identified as local minima. The success of the AFIR function is understandable by considering the FMO theory as illustrated in Section III using a very simple reaction $CO_2 + H \rightarrow HCO_2/HOCO$ as an example.

III. AN EXAMPLE OF LANDSCAPE OF THE AFIR FUNCTION

To illustrate a typical landscape of the AFIR function, we revisit a reaction of $CO_2 + H \rightarrow HCO_2/HOCO$. This reaction is the first step of $CO_2 + H \rightarrow CO + OH$ or the final step of the inverse $CO + OH \rightarrow CO_2 + H$.[87] Figure 3a shows an interaction potential energy contour map between a CO_2 molecule and a H atom at the B3LYP/cc-pVTZ level, where the positions of the C and O atoms in CO_2 were fixed at those of optimized CO_2. A similar contour map is reported in ref 87 with a different computation level. There are very shallow minima in the diagonal directions, probably because of the basis set superposition error. These minima are not important in chemical reactions.

Although all directions are almost completely repulsive, many chemists may recognize the reactive sites by looking at the FMOs of CO_2 shown in Figure 3b. The lowest unoccupied molecular orbitals (LUMOs) are degenerate π orbitals with a node on each C═O bond. The highest occupied molecular orbitals (HOMOs) of CO_2 are degenerate π orbitals with a node on the C atom. One reactive site should be the perpendicular direction (see the red arrow in Figure 3a) as LUMOs have the largest lobe toward this

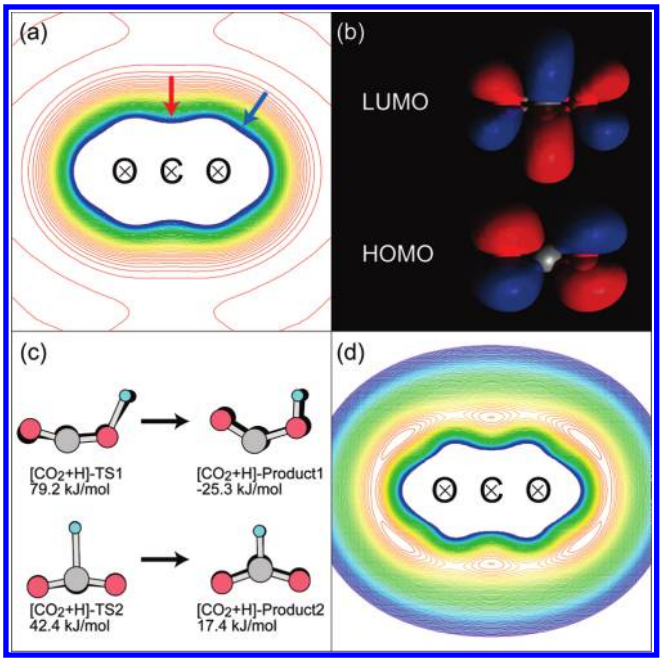

Figure 3. (a) The interaction potential contour map between a CO_2 molecule and a H atom at the B3LYP/cc-pVTZ level, where the contour spacing is 5 kJ/mol and reactive sites are indicated by arrows; (b) the FMOs of a CO_2 molecule at the same computation level; (c) true TS and product structures for the CO_2 + H reaction at the same level, where approximate TS and product structures along an AFIR path (see text for details) are shown behind the true structures with blackbody; and (d) the contour plot of the AFIR function with γ = 200 kJ/mol for the interaction between a CO_2 molecule and a H atom at the B3LYP/cc-pVTZ level.

direction. Another should be the diagonal direction (see the blue arrow in Figure 3a) because of the lobe of HOMOs in this direction. The interaction between these frontier orbitals and the 1s orbital of the H atom lowered the potential energy in these directions, and consequently, dents are seen in these directions in Figure 3a. Actually, the reaction has been found to take place when the H atom collides toward either of these dents (see TSs in Figure 3c).

If a function has local minima only in the reactive directions, then one can find them easily by minimizing the function. The AFIR function does have such a landscape as shown in Figure 3d, which is a contour plot of the AFIR function with γ = 200 kJ/mol (the second term of eq 2 is added to the plot of Figure 3a). The values of the AFIR function linearly decrease from the long distance to the medium distance because of the artificial force. In the short distance, the strong repulsion between two particles supersedes the artificial force, and the resulting potential curve has a minimum in the medium distance. There we see a clear angular dependence of the depth of the minimum and find local minima at the reactive sites. Once such a reactive site is found as a local minimum of the AFIR function, by increasing the γ value, one can find an approximate reaction path, along which approximate TS and product points can be obtained.

Figure 3c compares approximate AFIR structures with true TSs and true products, where AFIR structures obtained by the algorithm in Figure 2 with N_{MAX} = 10 and γ_{MAX} = 200 kJ/mol are shown in black behind the true stationary structures. The AFIR structures, especially the approximate TS structures, are quite

similar to the true ones. Moreover, all AFIR paths with different initial orientations gave one of these two unique reaction paths; there was no miss shot and no useless vibrations or fluctuations in the AFIR search. Before the completion of the algorithm, 564 gradients and 21 Hessian were computed in this application.

As seen in Figure 3a, the frontier (and other important) orbital interactions leading to chemical reactions should have significant effects on the repulsive potential walls. However, orbital interaction works in relatively short ranges compared to H-bond interaction as well as electrostatic and dispersion interactions. Hence, dents indicating entrances of reaction paths are not always seen clearly as local minima. By pressing the reactants to each other by the artificial force to accentuate such dents in the short-range (see Figure 3d), locations of maximal orbital interaction can be visualized as local minima so that the computer can detect them without extensive sampling or scans. Although the FMO theory itself is also very powerful in predictions of reactive sites, it does not work very well when many orbitals are involved at once or when changes in shapes and/or characters of FMOs are significant due to strong interactions with the collision partner. On the other hand, the AFIR method looks at the shape of PES avoiding these difficulties in the FMO theory.

IV. TEST CALCULATIONS

Aldol Reaction. As a case study, the reaction between vinyl alcohol ($H_2C{=}CH{-}OH$) and formaldehyde (H_2CO) was studied by the AFIR method. In this and the following applications, gradients and Hessians were computed at the B3LYP/6-31G level by the Gaussian09 program.[88] This calculation is expected to give the products of the aldol reaction. In the aldol reaction, vinyl alcohol is assumed to be an important intermediate which reacts with another reactant, an aldehyde molecule.[89] Hence, the most important point in this application is whether the AFIR method can find the product of aldol reaction or not. At γ_{MAX} = 100 kJ/mol, only one path was obtained, which is shown in Figure 4. In Figure 4 and others shown below, six structures are presented for each path: a starting random structure for the corresponding AFIR minimization, a reactant complex structure found by an IRC calculation from the corresponding true TS structure, a true TS structure, a highest energy structure along the corresponding AFIR path (shown in black behind the true TS structure for comparison), a true product structure found by an IRC calculation from the corresponding true TS structure, and a product structure with the corresponding AFIR path (shown in black behind the true product structure). The only path shown in Figure 4 actually corresponds to the final step of aldol reaction. As seen in the TS structure, the approximate structure along the AFIR path is quite similar to the true TS structure. The approximate product structure along the AFIR path is also similar to the true product structure. Thus, the AFIR method worked very well. In this application with N_{MAX} = 30, 33 random structures were considered, and 3490 gradient and 87 Hessian calculations were performed in total.

To find the higher barrier paths systematically, γ_{MAX} was set to a very large value of 1000 kJ/mol. All the obtained paths are listed in Figure 5. The order of the path ID numbers represents the order in which the structure was found in the AFIR search. The most important path leading to the aldol product was found first among the 13 paths. This is probably because the acceptance region of this path is much wider than the others because of the low barrier of this path. All the other paths have barriers higher

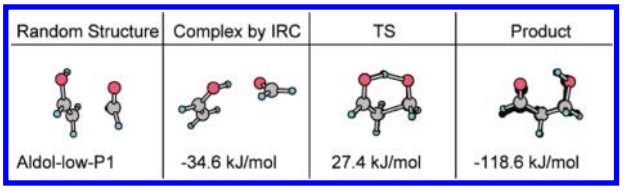

Figure 4. The reaction path between $H_2C{=}CH{-}OH$ and H_2CO obtained by the AFIR search with γ_{MAX} = 100 kJ/mol at the B3LYP/6-31G level. Six structures with their energies relative to the isolated reactants are presented: a starting randomly oriented structure as the starting point for the AFIR minimization, a reactant complex structure found by an IRC calculation from the corresponding true TS structure, a true TS structure, a highest energy structure along the corresponding AFIR path (shown in black behind the true TS structure for comparison), a true product structure found by an IRC calculation from the corresponding true TS structure, and a product structure along the corresponding AFIR path (shown in black behind the true product structure).

than 100 kJ/mol. Although deviations between approximate TS and true TS structures are large in some paths, these are still acceptable since in all cases geometry optimization by the RFO method starting from these approximate TS structures converged within 30 optimization steps to the true TS structures. However, in future applications, there may be cases in which optimization of a true TS geometry fails due to a very poor AFIR guess. In such cases, one of the double-end methods[11,12,37−42] could be applied to the corresponding pair of product and reactant. Besides these paths, many biradical hydrogen-transfer paths were obtained giving $H_2C{=}CH{-}O^{\bullet} + H_2{}^{\bullet}COH$, $H_2C{=}C^{\bullet}{-}OH + H_2{}^{\bullet}COH$, $H^{\bullet}C{=}CH{-}OH + H_2{}^{\bullet}COH$, $H_2C{=}CH{-}O^{\bullet} + H_3CO^{\bullet}$, $H_2C{=}C^{\bullet}{-}OH + H_3CO^{\bullet}$, $H^{\bullet}C{=}CH{-}OH + H_3CO^{\bullet}$, $H_2C{=}C^{\bullet}H\cdots OH_2 + H^{\bullet}CO$, $H_2{}^{\bullet}C{-}CH_2{-}OH + H^{\bullet}CO$, and $H_3C{-}{}^{\bullet}CH{-}OH + H^{\bullet}CO$. This result demonstrates that the AFIR method, with the combination of the AFIR function in eq 2 and the algorithm in Figure 2, has the ability to find many unknown paths automatically and systematically without prejudice toward assumed mechanisms. In this application with N_{MAX} = 50, 505 random structures were considered, and 59 208 gradient calculations and 1486 Hessian calculations were performed in total. As expected, the cost is much larger in this application than the above application with the small γ_{MAX} due to many high-barrier paths. One may choose to use a small γ_{MAX}, if high-barrier paths are not interested.

In the search with γ_{MAX} = 1000 kJ/mol, there were five unique AFIR paths that ended without any reaction. For completeness, these paths were further followed with γ = 5000 kJ/mol starting from these nonreacted end points, and all of these five finally reacted (see Figure S1 in Supporting Information for these additional five paths). In other words, there was no AFIR path that ran into a dead end valley in this particular example. The situation was the same also in the above example for CO_2 + H. As demonstrated for CO_2 + H in Figure 3, all reactive sites emerge as local minima on the AFIR function, which helped to automatically find effective coordinates to be driven by the artificial force also in the case of $H_2C{=}CH{-}OH + H_2CO$. One problem in the present algorithm is that each AFIR path is found again and again starting from many random orientations. In the case of the search with γ_{MAX} = 1000 kJ/mol, 27 unique paths were obtained from 505 orientations; each product was reached 18.7 times on average. It follows that most paths can be discarded in the course of the minimizations before they reach the products when some

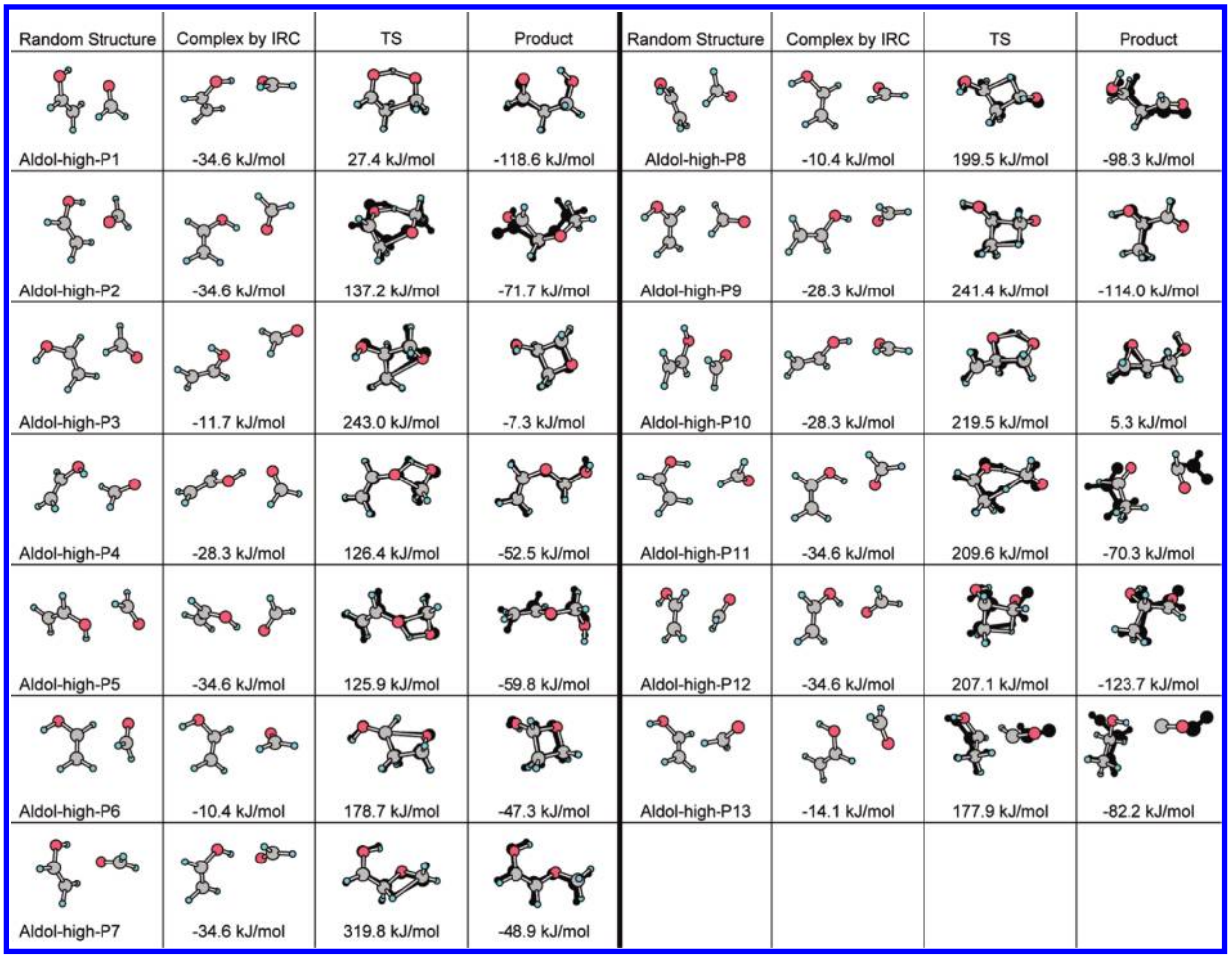

Figure 5. The reaction paths between $H_2C{=}CH{-}OH$ and H_2CO obtained by the AFIR search with γ_{MAX} = 1000 kJ/mol at the B3LYP/6-31G level. See the caption of Figure 4 for the meanings of each structure.

similarities are found between the present path and one of previous paths. This trick, once implemented, will reduce the total computation cost dramatically.

Aldol Reaction Catalyzed by a Single Water Molecule. As a case study of three component reactions, one water molecule is reacted together with $H_2C{=}CH{-}OH$ and H_2CO. In this application, in addition to the attraction between $H_2C{=}CH{-}OH$ and H_2CO, two more terms were added to eq 2, one for attraction between $H_2C{=}CH{-}OH$ and H_2O and the other between H_2CO and H_2O. We chose the same α for the three force terms, and thus the γ value is divided three in calculations of α with eq 3. It is possible to apply different α to each term, however, this is not recommended. As discussed above, one important role of the AFIR function is to accentuate intrinsic topography on potential walls of original PESs, as shown in Figure 3d. Not to destroy the anisotropy of the topography, the AFIR function should be as simple as possible.

All paths obtained by a search with γ_{MAX} = 100 kJ/mol is presented in Figure 6. There are two aldol paths with different conformations (W1−P2 and W1−P5). With participation of one water molecule, an analog of aldol-high-P4 in Figure 5, i.e., W1−P1 in Figure 6, was found with this small γ_{MAX}. Two new types of paths opened, giving methylene-diol with (W1−P6 and W1−P8) and without (W1−P3, W1−P4, and W1−P7) the enol−keto tautomerization. All the AFIR paths provided good approximate TS and product geometries also in this three-component system. In this application with N_{MAX} = 30, 97 random structures were considered, and 13 961 gradient and 340 Hessian calculations were performed in total.

Aldol Reaction Catalyzed by Two Water Molecules. In three component reactions among A, B, and C, the AFIR function having three force terms (for A−B, A−C, and B−C attractions) is unique. On the other hand, when four components A, B, C, and D are involved at once, there are six force terms for the A−B, A−C, A−D, B−C, B−D, and C−D attractions. One is the function with all six terms. However, such reactions giving at least six new chemical bonds in one step are highly unlikely. Hence, one needs to consider also AFIR functions with 3−5 force terms, which gives formally 38 possible force combinations. In addition to one six-term function above, there are six ($_6C_5$) five-term possibilities, 15 ($_6C_4$) four-term cases, and 16 ($_6C_3 - 4$, where the four cases involve an isolated component and are treated as three-component reactions) three-term cases. In a fully systematic search, one should consider all of these 38 possibilities. In the present case study, only one of such cases is studied, where A, B, C, and D are $H_2C{=}CH{-}OH$, H_2CO, H_2O, and H_2O, respectively, and the AFIR function consists of four terms for the A−B, A−C, B−D, and C−D attractions. This is expected to give reaction paths between $H_2C{=}CH{-}OH$ and H_2CO involving two H_2O molecules as proton-transfer agents. If we

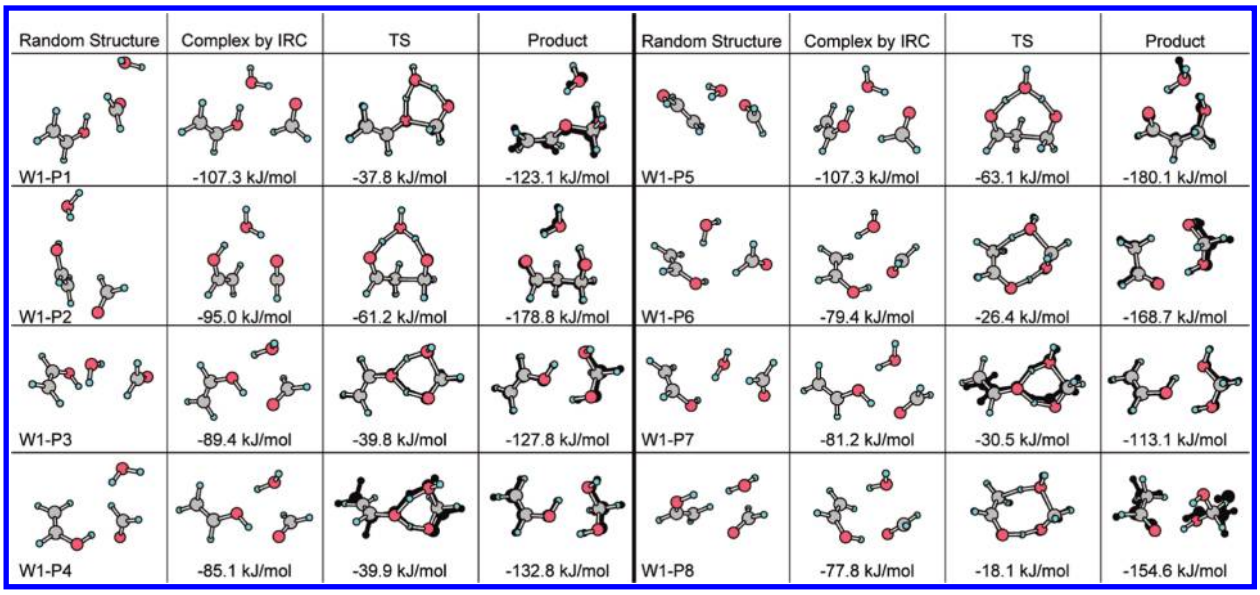

Figure 6. The reaction paths among $H_2C{=}CH{-}OH$, H_2CO, and H_2O obtained by the AFIR search with γ_{MAX} = 100 kJ/mol at the B3LYP/6-31G level. See the caption of Figure 4 for the meanings of each structure.

intend to investigate the catalytic role of two solvent molecules in a bimolecular reaction, then this is the unique choice among the 38 possibilities.

All paths obtained by a search with γ_{MAX} = 100 kJ/mol are presented in Figure 7. All products in Figure 7 are already seen in Figure 6, although in all paths, the second water molecule is explicitly involved as a proton-transfer agent. The AFIR paths again provided good estimates of TS and product geometries for full optimization. In this application with N_{MAX} = 30, 180 random structures were considered, and 29 508 gradient and 699 Hessian calculations were performed in total.

If Figures 4−7 are compared, then very large catalytic effects of the first and second water molecules are seen. However, the effects are significantly overestimated because of the basis set superposition errors of 6-31G. Figure 8 shows the aldol reaction paths at the B3LYP/cc-pVTZ level, where TSs were optimized starting from those for aldol-high/low-P1, W1−P5, and W2−P4. As shown in Figure 8, when the larger basis sets are employed, the energy lowering in relative potential energies is much smaller. Moreover, if standard-state free energies at room temperature are considered, participation of water molecules increases the barrier height. Hence, in gas phase, catalytic effects of water molecules are not important in this reaction.

V. CONCLUSIONS AND PERSPECTIVES

One goal in development of tools for exploring PESs would be establishing a general approach which can predict the entire sets of chemical reaction mechanisms automatically starting from a given set of reactants and catalysts. Such a method, once realized, will be very useful for exploring unknown chemical worlds by using computers. Toward this unachieved goal, we introduced the AFIR method for finding associative ($A + B \rightarrow X$) paths automatically. AFIR by pressing the reactants to each other with an artificial force can locate the reactive sites of each reactant very efficiently by accentuating the effects of (short-range) orbital interactions. Once such a reactive site is located, further pressing will lead to an approximate TS geometry and eventually to the product. This procedure can be performed very efficiently just by minimizing a single function called the AFIR function. Approximate TS and product geometries can then easily be reoptimized to corresponding true TS and product structures by geometry optimization without the artificial force.

One of the most successful approaches for recognizing reactive sites should be the FMO theory and the Woodward−Hoffmann rules.[33−36] Although these theories have been very powerful for explaining chemical reactivates, they have not been applied successfully to systematic predictions of reaction paths in combinations with quantum chemical calculations of PESs. Shapes of FMOs are known to change significantly by interaction with collision partners in some examples,[90,91] and hence, FMOs for isolated molecules are not always very useful in predicting reactive sites. To our knowledge, for this particular purpose, there has been no systematic theoretical approach beyond these theories. On the other hand, AFIR has the ability to predict the reactive sites with quantum chemical calculations of PESs. Moreover, AFIR can predict TS geometries in courses of the AFIR minimization.

There is another unique feature of AFIR to be noted. In most methods for finding reaction paths without a guess of TS geometry, many cycles of constrained/penalty function optimization or extensive PES sampling are required before obtaining a path. However, in AFIR, just minimization of one single function gives a path. On the AFIR function, there is a local minimum (or minima) at each reactive site. This has been illustrated in Figure 3d and is obvious from many reaction paths shown in Figures 4−7 that were obtained just by minimizing the AFIR functions. Hence, from a given initial orientation, the system is drawn into one of these sites. If a H atom is placed at any direction of Figure 3d, it will automatically fall into one of the reactive sites. This feature makes search for each single path very efficient. Consequently, the automated stochastic search for many paths was possible even with the brute-force algorithm in Figure 2. Improvements of the stochastic part of the algorithm in Figure 2 may increase the efficiency in the total automated searches in the future.

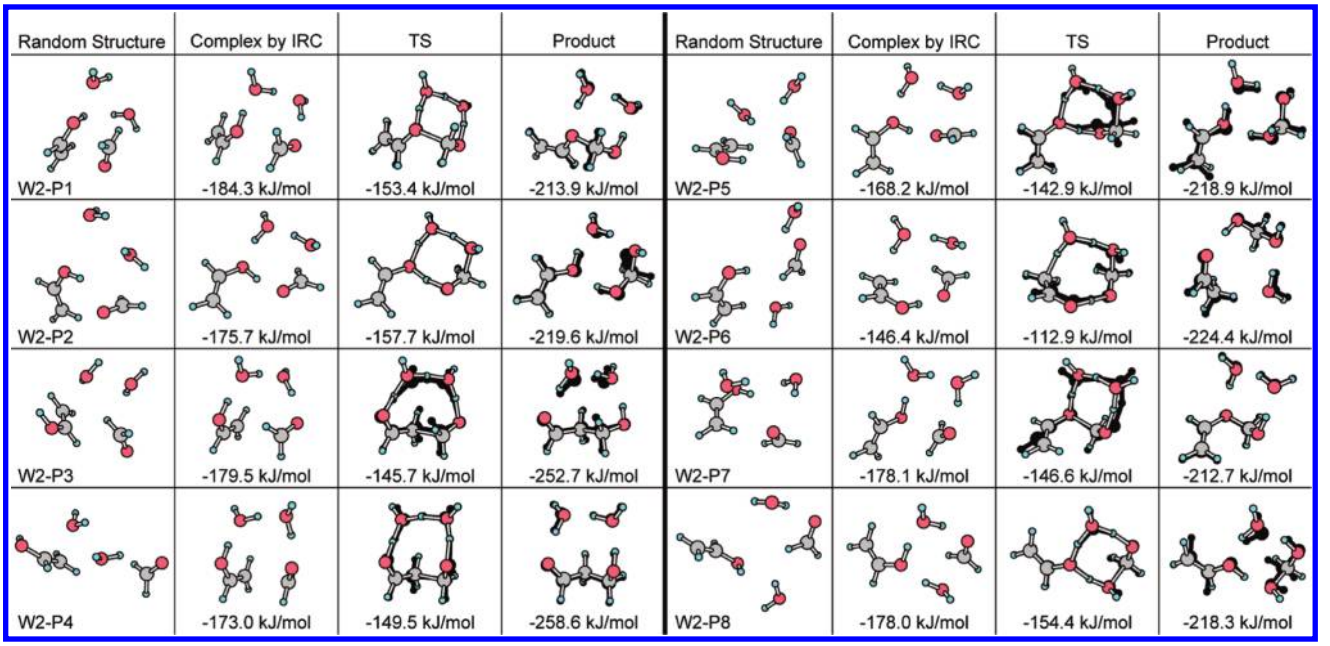

Figure 7. The reaction paths among $H_2C{=}CH{-}OH$, H_2CO, H_2O, and H_2O obtained by the AFIR search with γ_{MAX} = 100 kJ/mol at the B3LYP/6-31G level. See the caption of Figure 4 for the meanings of each structure.

We note that the AFIR search should be performed for all important conformers when reactants have several conformers. Small conformational changes may occur during AFIR minimization as seen in P4, P9, and P10 in Figure 5. However, for many reaction paths the conformation does not change. Therefore all the conformations need to be considered for the search. Hence, we suggest to perform conformation sampling for reactants before the AFIR search. Many previous researches are available regarding the expansion of the applicability of reaction path search methods to larger complex systems; see refs 92−96 for most successful examples for the EF and NEB methods. Their strategies may be helpful in future applications of AFIR to complex reactions.

In multistep mechanisms, unimolecular steps may also be involved. It is still under tests how well AFIR can be applied to unimolecular reactions. As discussed in the Introduction, some methods are already available for unimolecular paths. Among them, the ADDF method has been demonstrated to be very powerful for local chemical bond rearrangements.[64−68] Hence, we believe that the goal of finding total chemical reaction mechanisms automatically starting from given reactants and catalysts will be achieved in the future by a combination of AFIR for A + B → X (+ Y) steps and ADDF (or others) for A → X (+ Y) steps.

There are some useful techniques to make applications of automated reaction path search methods to large flexible systems and to nonadiabatic (photochemical, ion−molecule, and spin-flipping) reactions.[69,70] Although these techniques were originally introduced in a combination with the ADDF method, in principle they can be combined with any automated reaction path search method including AFIR. One of such techniques is the microiteration technique used in QM/MM geometry optimization.[97−99] With microiteration and the effective Hessian approach, reaction paths concerned within a given reaction center can be explored automatically.[69] This technique is expected to greatly expand the applicability of AFIR to larger molecular systems. The development combining AFIR and microiteration within the ONIOM(QM:MM)[100] framework has already been done, and systematic tests are in progress for an organometallic catalytic reaction with flexible ligands. This approach is expected to develop into applications of AFIR to enzymatic reactions. In enzymatic reactions as well as reactions in solution phase, thermal entropy effects play a significant role. To account for the entropy efficiently, several powerful free energy methods are available, such as umbrella sampling,[101] metadynamics,[44] free energy perturbation theory,[102] etc. Development of interfaces with these free energy methods will be a very important subject in the future.

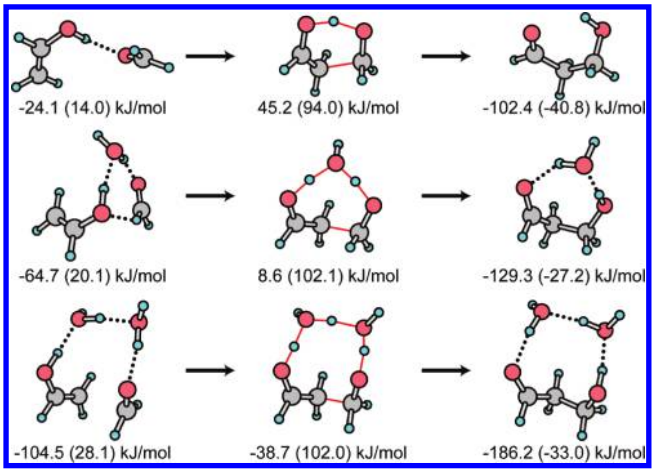

Figure 8. The aldol reaction paths involving zero to two water molecules at the B3LYP/cc-pVTZ level. Values in parentheses show relative standard-state free energies at room temperature.

Another such technique is the seam model function (SMF) approach for nonadiabatic reactions. In the SMF approach, many minima on seam of crossing hypersurfaces (MSXs) are searched in two steps: automated exploration of many approximate MSX

structures using a penalty function by an automated reaction path search method, followed by tight MSX optimization using the approximate structures and an accurate MSX optimizer.[70] Here, "seam of crossing" includes conical intersections between states with the same spin and space symmetry. With SMF and ADDF, photodissociation mechanisms of small atmospheric species have been investigated systematically.[70,103−106] We already combined SMF with AFIR and applied to exploration of nonadiabatic ignition pathways of unsaturated hydrocarbons.[75] In this application, we discovered unexpected ignition pathways through low-energy MSXs for aromatic hydrocarbons. Thus, applications of the automatic search method to photochemical, ion−molecule, and spin-flipping reactions are also possible. Interfaces with free energy methods as well as microiteration will be required also in this extension for nonadiabatic reactions in the future.

In these five decades, computational chemistry has become a powerful means for exploration of chemical worlds in collaboration with experiments. In many studies of chemical reactions, it has been a splendid guide to confirm or to judge ideas of computational and/or experimental chemists through the use of sophisticated PES exploration tools. One of the important subjects in the next generation should be predicting reaction paths without presumed mechanisms. This has been achieved at least for reactions of type A + B → X (+ Y) in small systems by the present AFIR method. Obviously, further development of automated reaction path search methods will be required in the future to cover reactions of many kinds in a variety of system size.

■ ASSOCIATED CONTENT

Supporting Information. Additional five pathways for $H_2C{=}CH{-}OH{+}H_2CO$. This material is available free of charge via the Internet at http://pubs.acs.org.

■ AUTHOR INFORMATION

Corresponding Authors

*E-mail: keiji.morokuma@emory.edu; smaeda@fukui.kyoto-u.ac.jp.

■ ACKNOWLEDGMENT

This work is partly supported by a grant from Japan Science and Technology Agency with a Core Research for Evolutional Science and Technology (CREST) in the Area of High Performance Computing for Multiscale and Multiphysics Phenomena at Kyoto University as well as a grant from US AFOSR (grant no. FA9550-10-1-0304) at Emory University. S.M. thanks Prof. Koichi Ohno of Toyota Physical and Chemical Research Institute for helpful discussions and comments as well as his guidance on the reaction path search problem. We thank Prof. Masanobu Uchiyama of RIKEN and The University of Tokyo for helpful discussions and comments in the development. S.M. thanks Dr. Steven K. Burger of McMaster University for helpful discussions about reaction path search methods.

■ REFERENCES

(1) Glasstone, S.; Laidler, K.; Eying, H. *The Theory of Rate Processes*; McGraw-Hill: New York, 1941.
(2) Murrell, J. N.; Laidler, K. J. *Trans. Faraday Soc.* **1968**, *64*, 371–377.
(3) Brown, A.; Dewar, M. J. S.; Schoeller, W. *J. Am. Chem. Soc.* **1970**, *92*, 5516–5517.
(4) McIver, J. W., Jr.; Komornicki, A. *J. Am. Chem. Soc.* **1972**, *94*, 2625–2633.
(5) Hayes, D. M.; Morokuma, K. *Chem. Phys. Lett.* **1972**, *12*, 539–543.
(6) Jaffe, R. L.; Hayes, D. M.; Morokuma, K. *J. Chem. Phys.* **1974**, *60*, 5108–5109.
(7) Fukui, K. *J. Phys. Chem.* **1970**, *74*, 4161–4163.
(8) Ishida, K.; Morokuma, K.; Komornicki, A. *J. Chem. Phys.* **1977**, *66*, 2153–2156.
(9) Pulay, P. *Mol. Phys.* **1969**, *17*, 197–204.
(10) Komornicki, A.; Ishida, K.; Morokuma, K.; Ditchfield, R.; Conrad, M. Efficient. *Chem. Phys. Lett.* **1977**, *45*, 595–602.
(11) Schlegel, H. B. *J. Comput. Chem.* **2003**, *24*, 1514–1527.
(12) Jensen, F. *Introduction to Computational Chemistry*, 2nd ed.; Wiley: Chichester, U.K., 2007.
(13) Koga, N.; Morokuma, K. *Chem. Rev.* **1991**, *91*, 823–842.
(14) Niu, S.; Hall, M. B. *Chem. Rev.* **2000**, *100*, 353–405.
(15) Ziegler, T.; Autschbach, J. *Chem. Rev.* **2005**, *105*, 2695–2722.
(16) Houk, K. N.; Cheong, P. H.-Y. *Nature* **2008**, *455*, 309–313.
(17) Wales, D. J.; Scheraga, H. A. *Science* **1999**, *285*, 1368–1372.
(18) Floudas, C. A.; Pardalos, P. M. *Optimization in Computational Chemistry and Molecular Biology: Local and Global Approaches*, Kluwer Academic Publishers: Dordrecht, The Netherlands, 2000.
(19) Dobson, C. M.; Šali, A.; Karplus, M. *Angew. Chem., Int. Ed.* **1998**, *37*, 868–893.
(20) Wales, D. J. *Int. Rev. Phys. Chem.* **2006**, *25*, 237–282.
(21) Dill, K. A.; Ozkan, S. B.; Shell, M. S.; Weikl, T. R. *Annu. Rev. Biophys.* **2008**, *37*, 289–316.
(22) Maddox, J. *Nature* **1988**, *335*, 201–201.
(23) Woodley, S. M.; Catlow, R. *Nat. Mater.* **2008**, *7*, 937–946.
(24) Müller, K.; Brown, L. D. *Theor. Chim. Acta* **1979**, *53*, 75–93.
(25) Page, M.; McIver, J. W., Jr. *J. Chem. Phys.* **1988**, *88*, 922–935.
(26) Gonzalez, C.; Schlegel, H. B. *J. Chem. Phys.* **1989**, *90*, 2154–2161.
(27) Hratchian, H. P.; Schlegel, H. B. *J. Chem. Theory Comput.* **2005**, *1*, 61–69.
(28) Schlegel, H. B. *J. Comput. Chem.* **1982**, *3*, 214–218.
(29) Farkas, Ö.; Schlegel, H. B. *J. Chem. Phys.* **1999**, *111*, 10806–10814.
(30) Cerjan, C. J.; Miller, W. H. *J. Chem. Phys.* **1981**, *75*, 2800–2801.
(31) Császár, P.; Pulay, P. *J. Mol. Struct.* **1984**, *114*, 31–34.
(32) Banerjee, A.; Adams, N.; Simons, J.; Shepard, R. *J. Phys. Chem.* **1985**, *89*, 52–57.
(33) Fukui, K.; Yonezawa, T.; Shingu, H. *J. Chem. Phys.* **1952**, *20*, 722–725.
(34) Fukui, K. *Acc. Chem. Res.* **1971**, *4*, 57–64.
(35) Woodward, R. B.; Hoffmann, R. *J. Am. Chem. Soc.* **1965**, *87*, 395–397.
(36) Woodward, R. B.; Hoffmann, R. *Angew. Chem., Int. Ed.* **1969**, *8*, 781–853.
(37) Halgren, T. A.; Lipscomb, W. N. *Chem. Phys. Lett.* **1977**, *49*, 225–232.
(38) Dewar, M. J. S.; Healy, E. F.; Stewart, J. J. P. *J. Chem. Soc., Faraday Trans. 2* **1984**, *80*, 227–233.
(39) Elber, R.; Karplus, M. *Chem. Phys. Lett.* **1987**, *139*, 375–380.
(40) Henkelman, G.; Uberuaga, B. P.; Jónsson, H. *J. Chem. Phys.* **2000**, *113*, 9901–9904.
(41) E, W.; Ren, W.; Vanden-Eijnden, E. *Phys. Rev. B* **2002**, *66*, 052301/1–4.
(42) Peters, B.; Heyden, A.; Bell, A. T.; Chakraborty, A. *J. Chem. Phys.* **2004**, *120*, 7877–7886.
(43) Černohorský, M.; Kettou, S.; Koča, J. *J. Chem. Inf. Comput. Sci.* **1999**, *39*, 705–712.
(44) Laio, A.; Parrinello, M. *Proc. Natl. Acad. Sci. U.S.A.* **2002**, *99*, 12562–12566.
(45) Ensing, B.; De Vivo, M.; Liu, Z.; Moore, P.; Klein, M. L. *Acc. Chem. Res.* **2006**, *39*, 73–81.
(46) Burger, S. K.; Ayers, P. W. *J. Chem. Theory Comput.* **2010**, *6*, 1490–1497.

(47) Pancíř, J. *Collect. Czech. Chem. Commun.* **1974**, *40*, 1112–1118.
(48) Basilevsky, M. V.; Shamov, A. G. *Chem. Phys.* **1981**, *60*, 347–358.
(49) Basilevsky, M. V. *Chem. Phys.* **1982**, *67*, 337–346.
(50) Rowe, D. J.; Ryman, A. *J. Math. Phys.* **1982**, *23*, 732–735.
(51) Hoffman, D. K.; Nord, R. S.; Ruedenberg, K. *Theor. Chim. Acta* **1986**, *69*, 265–279.
(52) Jørgensen, P.; Jensen, H. J. A.; Helgaker, T. *Theor. Chim. Acta* **1988**, *73*, 55–65.
(53) Quapp, W. *Theor. Chim. Acta* **1989**, *75*, 447–460.
(54) Schlegel, H. B. *Theor. Chim. Acta* **1992**, *83*, 15–20.
(55) Sun, J.-Q.; Ruedenberg, K. *J. Chem. Phys.* **1993**, *98*, 9707–9714.
(56) Bondensgård, K.; Jensen, F. *J. Chem. Phys.* **1996**, *104*, 8025–8031.
(57) Quapp, W.; Hirsch, M.; Imig, O.; Heidrich, D. *J. Comput. Chem.* **1998**, *19*, 1087–1100.
(58) Quapp, W.; Hirsch, M.; Heidrich, D. *Theor. Chem. Acc.* **1998**, *100*, 285–299.
(59) Bofill, J. M.; Anglada, J. M. *Theor. Chem. Acc.* **2001**, *105*, 463–472.
(60) Crehuet, R.; Bofill, J. M.; Anglada, J. M. *Theor. Chem. Acc.* **2002**, *107*, 130–139.
(61) Dallos, M.; Lischka, H.; Monte, E. V. D.; Hirsch, M.; Quapp, W. *J. Comput. Chem.* **2002**, *23*, 576–583.
(62) Hirsch, M.; Quapp, W. *J. Comput. Chem.* **2002**, *23*, 887–894.
(63) Hirsch, M.; Quapp, W. *J. Mol. Struct. (Theochem)* **2004**, *683*, 1–13.
(64) Ohno, K.; Maeda, S. *Chem. Phys. Lett.* **2004**, *384*, 277–282.
(65) Maeda, S.; Ohno, K. *J. Phys. Chem. A* **2005**, *109*, 5742–5753.
(66) Ohno, K.; Maeda, S. *J. Phys. Chem. A* **2006**, *110*, 8933–8941.
(67) Ohno, K.; Maeda, S. *Phys. Scr.* **2008**, *78*, 058122/1–8.
(68) Maeda, S.; Ohno, K. *J. Phys. Chem. A* **2007**, *111*, 4527–4534.
(69) Maeda, S.; Ohno, K.; Morokuma, K. *J. Chem. Theory Comput.* **2009**, *5*, 2734–2743.
(70) Maeda, S.; Ohno, K.; Morokuma, K. *J. Phys. Chem. A* **2009**, *113*, 1704–1710.
(71) Irikura, K. K.; Johnson, R. D., III *J. Phys. Chem. A* **2000**, *104*, 2191–2194.
(72) Müller, E. M.; de Meijere, A.; Grubmüller, H. *J. Chem. Phys.* **2002**, *116*, 897–905.
(73) Maeda, S.; Morokuma, K. *J. Chem. Phys.* **2010**, *132*, 241102/1–4.
(74) Maeda, S.; Komagawa, S.; Uchiyama, M.; Morokuma, K. *Angew. Chem., Int. Ed.* **2011**, *50*, 644–649.
(75) Maeda, S.; Saito, R.; Morokuma, K. *J. Phys. Chem. Lett.* **2011**, *2*, 852–857.
(76) Collins, M. A. *Theor. Chem. Acc.* **2002**, *108*, 313–324.
(77) Culot, P.; Dive, G.; Nguyen, V. H.; Ghuysen, J. M. *Theor. Chim. Acta.* **1992**, *82*, 189–205.
(78) Broyden, C. G. *J. Inst. Math. Appl.* **1970**, *6*, 76–90.
(79) Fletcher, R. *Comput. J. (Switzerland)* **1970**, *13*, 317–322.
(80) Goldfarb, D. *Math. Comput.* **1970**, *24*, 23–26.
(81) Shanno, D. F. *Math. Comput.* **1970**, *24*, 647–656.
(82) Crippen, G. M.; Scheraga, H. A. *Proc. Natl. Acad. Sci. U.S.A.* **1969**, *64*, 42–49.
(83) Piela, L.; Kostrowick, J.; Scheraga, H. A. *J. Phys. Chem.* **1989**, *93*, 3339–3346.
(84) Huber, T.; Torda, A. E.; van Gunsteren, W. E. *J. Comput.-Aided Mol. Des.* **1994**, *8*, 695–708.
(85) Grubmüller, H. *Phys. Rev. E* **1995**, *52*, 2893–2906.
(86) Phillips, J. C.; Braun, R.; Wang, W.; Gumbart, J.; Tajkhorshid, E.; Villa, E.; Chipot, C.; Skeel, R. D.; Kalé, L.; Schulten, K. *J. Comput. Chem.* **2005**, *26*, 1781–1802.
(87) Schatz, G. C.; Fitzcharles, M. S.; Harding, L. B. *Faraday Discuss. Chem. Soc.* **1987**, *84*, 359–369.
(88) Frisch, M. J.; Trucks, G. W.; Schlegel, H. B.; Scuseria, G. E.; Robb, M. A.; Cheeseman, J. R.; Scalmani, G.; Barone, V.; Mennucci, B.; Petersson, G. A.; Nakatsuji, H.; Caricato, M.; Li, X.; Hratchian, H. P.; Izmaylov, A. F.; Bloino, J.; Zheng, G.; Sonnenberg, J. L.; Hada, M.; Ehara, M.; Toyota, K.; Fukuda, R.; Hasegawa, J.; Ishida, M.; Nakajima, T.; Honda, Y.; Kitao, O.; Nakai, H.; Vreven, T.; Montgomery, J. A., Jr.; Peralta, J. E.; Ogliaro, F.; Bearpark, M.; Heyd, J. J.; Brothers, E.; Kudin, K. N.; Staroverov, V. N.; Kobayashi, R.; Normand, J.; Raghavachari, K.; Rendell, A.; Burant, J. C.; Iyengar, S. S.; Tomasi, J.; Cossi, M.; Rega, N.; Millam, J. M.; Klene, M.; Knox, J. E.; Cross, J. B.; Bakken, V.; Adamo, C.; Jaramillo, J.; Gomperts, R.; Stratmann, R. E.; Yazyev, O.; Austin, A. J.; Cammi, R.; Pomelli, C.; Ochterski, J. W.; Martin, R. L.; Morokuma, K.; Zakrzewski, V. G.; Voth, G. A.; Salvador, P.; Dannenberg, J. J.; Dapprich, S.; Daniels, A. D.; Farkas, O.; Foresman, J. B.; Ortiz, J. V.; Cioslowski, J.; Fox, D. J. *Gaussian 09*, revision A.2; Gaussian, Inc.: Wallingford, CT, 2009.
(89) Kürti, L.; Czakó, B. Aldol Reaction. In *Strategic Applications of Named Reactions in Organic Synthesis*; Elsevier B.V.: Amsterdam, The Netherlands, 2005; pp 8−9.
(90) Fukui, K.; Koga, N.; Fujimoto, H. *J. Am. Chem. Soc.* **1981**, *103*, 196–197.
(91) Fukui, K. *Science* **1982**, *218*, 747–754.
(92) Munro, L. J.; Wales, D. J. *Phys. Rev. B* **1999**, *59*, 3969–3980.
(93) Henkelman, G.; Jónsson, H. *J. Chem. Phys.* **1999**, *111*, 7010–7022.
(94) Trygubenko, S. A.; Wales, D. J. *J. Chem. Phys.* **2004**, *120*, 2082–2094.
(95) Carr, J. M.; Trygubenko, S. A.; Wales, D. J. *J. Chem. Phys.* **2005**, *122*, 234903/1–7.
(96) Sheppard, D.; Terrell, R.; Henkelman, G. *J. Chem. Phys.* **2008**, *128*, 134106/1–10.
(97) Maseras, F.; Morokuma, K. *J. Comput. Chem.* **1995**, *16*, 1170–1179.
(98) Vreven, T.; Morokuma, K.; Farkas, Ö.; Schlegel, H. B.; Frisch, M. J. *J. Comput. Chem.* **2003**, *24*, 760–769.
(99) Vreven, T.; Frisch, M. J.; Kudin, K. N.; Schlegel, H. B.; Morokuma, K. *Mol. Phys.* **2006**, *104*, 701–714.
(100) Svensson, M.; Humbel, S.; Froese, R. D. J.; Matsubara, T.; Sieber, S.; Morokuma, K. *J. Phys. Chem.* **1996**, *100*, 19357–19363.
(101) Torrie, G. M.; Valleau, J. P. *J. Comput. Phys.* **1977**, *23*, 187–199.
(102) Hu, H.; Yang, W. *Annu. Rev. Phys. Chem.* **2008**, *59*, 573–601.
(103) Zhang, P.; Maeda, S.; Morokuma, K.; Braams, B. J. *J. Chem. Phys.* **2009**, *130*, 114304/1–10.
(104) Maeda, S.; Ohno, K.; Morokuma, K. *J. Phys. Chem. Lett.* **2010**, *1*, 1841–1845.
(105) Nádasdi, R.; Zügner, G. L.; Farkas, M.; Dóbé, S.; Maeda, S.; Morokuma, K. *ChemPhysChem* **2010**, *11*, 3883–3895.
(106) Xiao, H.; Maeda, S.; Morokuma, K. *J. Phys. Chem. Lett.* **2011**, *2*, 934–938.